THE EFFECT OF TANTALUM CONTENT ON MICROSTRUCTURE AND VICKERS HARDNESS OF TiNbZrTaAg ALLOY

Gabriel DOBRI[1], Andrei BERBECARU[2], Alexandru PARASCHIV[3] Victor GEANTA[2], Sorin CIUCA[2], Alexandra BANU[1]

Usually alloys from the titanium-niobium-zirconium-tantalum (TNZT) do not have intrinsic antibacterial properties and to induce such properties introducing alloying elements (silver, in this case) such property can be induced. This research is aimed at studying the influence of tantalum concentration variation on the microstructure of as cast alloys from the TNZT system with 2% silver addition.

The alloys were obtained by vacuum-arc remelting (VAR) and characterized by light and scanning electron microscopy, X-Ray diffraction and Vickers hardness tests. The studies are performed on as cast ingots, the intended use for the alloy being dentistry applications.

The alloy density was also determined using the water displacement method, the highest tantalum concentration (20%) resulting on a density of 6.87±0.01g/cm^3.

The results showed that the addition of tantalum increases β-phase content, generates a change in α-phase morphology and increases hardness starting from 15%wt.

Keywords: TNZT, microstructure, morphology, Vickers hardness, SEM

1. Introduction

The research for new materials for medical applications is ongoing since the characteristics of such materials are numerous: along those necessary in load bearing applications (mechanical characteristics), requirements for biocompatibility, biofunctionality and in specific cases biodegradability are added.

The summation of all requirements above, mandatory for materials used for implantable devices, in one single material is currently impossible and perpetual research in developing a material to satisfy a large number of criteria is ongoing. Currently there are several materials that have proven their viability as biomaterials [1], and as metallic materials consecrated are the stainless steels,

[1] The Faculty of Industrial Engineering and Robotics, University POLITEHNICA of Bucharest, Romania, e-mail: gabriel.dobri@upb.ro
[2] Materials Science and Engineering Faculty, University POLITEHNICA of Bucharest, Romania
[3] Department of Gas Turbines Special Components, COMOTI - R&D Romanian Institute, Bucharest, Romania,

cobalt - chromium alloys and titanium and its alloys. Each class comes with its own series of advantages and disadvantages: stainless steels have better fatigue resistance and ductility when compared with Co-Cr and Ti and its alloys, but they are the least biocompatible. The Co-Cr alloys stand out due to their good wear resistance, while Ti and its alloys are used for their biocompatibility and specific mechanical properties [2].

A major problem encountered for all metallic materials is the high density (when compared with bone density) and incompatibility with the mechanical properties of the bone. The main issue regarding the mechanical properties is the high elastic modulus of metallic materials (190-210GPa for stainless steels [2], 220GPa for Co-Cr alloys [2] and 90-110GPa for Ti and its alloys [2]) in respect to the one of the bone (10-40GPa, depending on health [3]) that shifts load distribution towards the implant, generates stress shielding and as consequence the bone loses its normal structure and properties [4].

Lowering the elastic modulus by changing the chemical composition can be achieved only for titanium alloys: titanium has an allotropic transformation at 880°C, below this temperature its crystal structure is hexagonal close - packed (described as α or α phase), and above the structure changes into a body centered cubic structure (described as α or β phase) [5]. The β phase has a low elastic modulus, and, although unstable at room temperature, it can be stabilized by the addition of specific alloying elements (the so called β stabilizers) as: V, Nb, Mo, Ta, Fe, Mn, Cr, Co, W, Ni, Cu, Si [6].

For medical applications Ti6Al4V has been used since 1960 and gradually replacing commercial-pure titanium due to its enhanced mechanical properties. The structure of the alloy is a mixture of (α+ β) phases, with an elastic modulus of roughly 110GPa. The high elastic modulus associated with presence of V and Al that are considered to be toxic in elemental state and as oxides [7] has directed the research towards β titanium alloys with safer (less toxic) alloying elements: Nb, Mo and Ta [8, 9]. A new element gained interest for its use in β titanium alloys, Zr: it has been found to help stabilize the phase of Ti when associated with another stabilizing element and contributing in a large extent to the descries of the elastic modulus.

The alloys from the titanium - niobium - tantalum - zirconium system (TNZT) gained interest given the good mechanical properties, low elastic modulus, good biocompatibility and corrosion resistance and are considered to be candidates for next-generation metallic biomaterials [10].

Intramedullary rods made of Ti-29Nb-13Ta-4.6Zr were already used for fracture fixation and spinal implants [11, 12] with outstanding success, Ti-35Nb-2Ta-3Zr [13] and Ti-29Nb-2Ta-3Zr [14] for dental implants, all with outstanding results.

A new trend arises in inducing antibacterial properties to the material, i.e. the ability of the material to remain effective under the action of bacteria and microorganisms, by addition of elements that can generate such behavior. For beta titanium alloys Shi et al. [15] obtained a low elastic modulus with good antibacterial properties given by the addition of copper, and others induced antibacterial properties by surface treatments [16-20].

A study performed by Kawakami [21] reveals that a great number of potential alloying elements are available that should induce antibacterial properties to be available, and yet to be studied in relation to TNZT alloys.

Adding silver to titanium alloys was attempted by Oh et al. [22] with good results up to 1.5%Ag, while most research studies were directed at surface modifications [23-27].

The current research state creates an opportunity for the development of an alloy in the TNZT system that includes silver for antibacterial properties which to be studied regarding the as cast microstructure, since the alloy is aimed for dental application.

2. Materials and methods

As the study was aimed at observing the influence of tantalum concentration on the as cast microstructure of a titanium alloy from the Titanium - Niobium - Zirconium - Tantalum, the remainder of alloying elements (Nb and Zr) had fixed concentrations as well as Ag.

The desired chemical compositions are presented in table 1, along with sample coding used throughout the paper.

Table 1

The aimed chemical composition of the alloys (in %wt)

Alloy code	%Ta	%Nb	%Zr	%Ag	%Ti
A1	0	9	8	2	Balance
A2	5	9	8	2	
A3	10	9	8	2	
A4	15	9	8	2	
A5	20	9	8	2	

The alloys were prepared in a vacuum arc remelting furnace (VAR) ABD MRF 900.

In order to obtain a good homogeneity of the experimental alloys nine passes were performed for each ingot. Each ingot has 10mm in diameter and a length of 150mm.

The obtained alloys were characterized first by determining the density using the water displacement method using ASTM D792 as guide for the procedure. The chemical composition of the experimental alloys was determined,

at this current stage, by Energy Dispersive X-Ray Spectroscopy (EDS) simultaneously with Scanning Electron Microscopy (SEM) observations using the FEI Inspect F50. The light microscopy studies were performed using a Reichert Univar microscope.

Mechanical characteristics were appreciated by performing Vickers Hardness tests using a Shimadzu HMV 2TE with a load of 1.961N and a holding time of 15s, following the specifications of ISO 6507-1.

3. Results and discussion

3.1. The density of the experimental alloys

The density of the experimental alloys was determined using the water displacement method using a graduated measuring cylinder to find the volume of the sample and an analytical scale for weight measurements. The density was determined by computing the ratio sample weight/sample volume. All measurements were repeated 5 times, then the average value and standard deviation were computed.

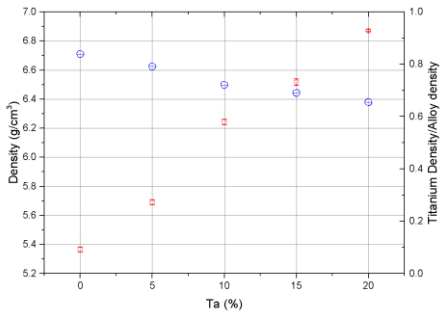

Fig. 1 The density of the experimental alloys in respect to tantalum concentration

In fig. 1 the density variation in respect to tantalum concentration is depicted.

The density appears to vary in a linear way increasing with the increase of tantalum concentration. Compared to pure titanium density (4.5g/cm3) these alloys show an increase in the range of 20-52%, as for the addition of tantalum to the base alloy (A1) an increase of maximum 27.22% was reached (for alloy A5).

The density increases limit the usability of these alloys to small components, yet their density is lower than those of 316L (8.0g/cm3) and cobalt-chromium alloys (10.0g/cm3).

3.2. The chemical composition of the experimental alloys

The chemical composition was estimated at this stage of the research, using EDS. On each sample 7 random fields were examined globally, using as guidelines a procedure recommended by Pencea et al. [28] to ensure that the samples have a homogeneous chemical composition. The analysis was mainly directed towards the concentrations of the alloying elements of interest. In table 2 the average concentrations of the alloying elements are presented.

Table 2

Determined chemical composition of the experimental alloys (%wt)

Alloy	%Ta	%Nb	%Zr	%Ag	%Ti
A1	Not Available	9.15±0.37	8.19±0.23	1.90±0.15	80.76±0.55
A2	3.95±0.30	7.52±0.56	6.87±0.35	1.96±0.08	79.71±1.03
A3	8.94±0.36	10.01±0.71	7.78±0.37	1.95±0.08	71.32±1.02
A4	15.58±0.51	9.32±0.25	7.68±0.23	1.86±0.08	65.55±0.63
A5	19.32±1.31	10.25±2.13	8.56±1.18	2.62±1.19	59.25±3.32

The chemical composition falls close to the desired one, although several discrepancies are present that should be reduced by optimizing the initial load of the melt.

3.3. The microstructure of the alloys

The prepared specimens were examined using the Reichert Univar light microscope. The representative micrographs are presented in fig. 2. An attempt to quantify constituent proportions by image analysis was performed using the Image-Pro Plus 6.0 (Media Cybernetics, Inc.) software, also used for various measurements.

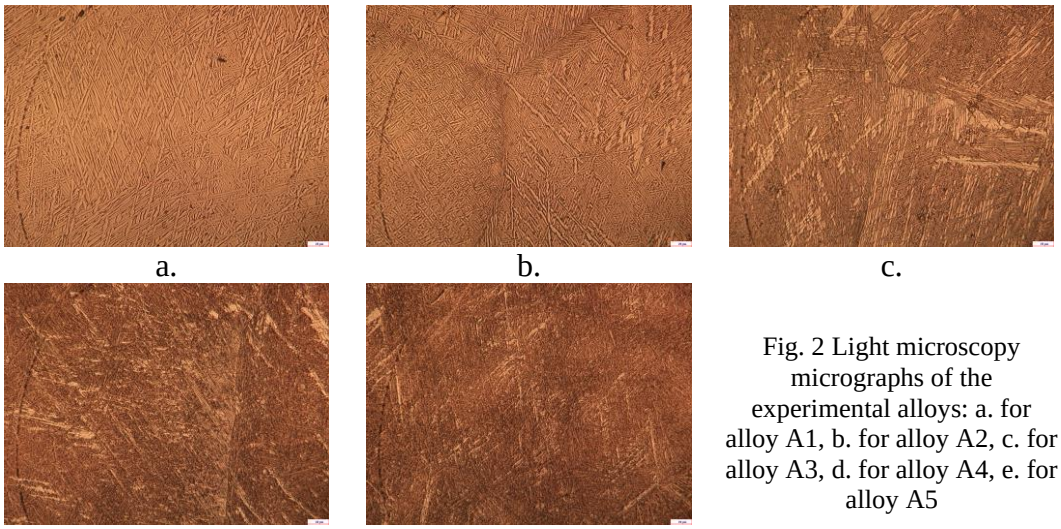

a. b. c. d. e.

Fig. 2 Light microscopy micrographs of the experimental alloys: a. for alloy A1, b. for alloy A2, c. for alloy A3, d. for alloy A4, e. for alloy A5

The microstructure of alloy A1, with no tantalum addition is depicted in fig. 2. a., showing a typical basket weave (or Widmanstatten) microstructure comprised of a mixture of α and β phases, with thick α lamellae, without preferred orientation, structure similar to a typical Ti6Al4V alloy [5,29-33]. By the addition of tantalum in alloy A1 no significant changes in the morphology can be assessed in fig. 2. b., the grain boundary of former β phase can be observed with α lamellae

present at this region. As tantalum content was further increased in alloy A3 the microstructure shows a significant change, as observed in fig. 2. c., the basket weave morphology disappears being substituted by an increasing β phase proportion and α phase morphology changes to lamellae colonies concentrated at prior β grain boundaries. The microstructure of alloy A4 presented in fig. 2. d. reveals a structure comprised of mostly β phase with α lamellae colonies present at former β grain boundaries. The highest tantalum content which was added in alloy A5 further reduces the α phase content, in fig. 2.d. a structure comprised mostly of β phase can be observed and fine α lamellae distributed as a star shape. The tantalum addition clearly alters the microstructure of the base alloy, starting from a α+β typical Widmanstatten structure towards a β structure with fine α lamellae distributed as colonies or as rosettes.

The structure of titanium alloys is dictated by alloying elements addition and processing route [5]. Regarding the experimental alloys, the factors that dictate the microstructure are: the chemical composition and the cooling rate (it cannot be excluded, although same parameters were used for all alloys).

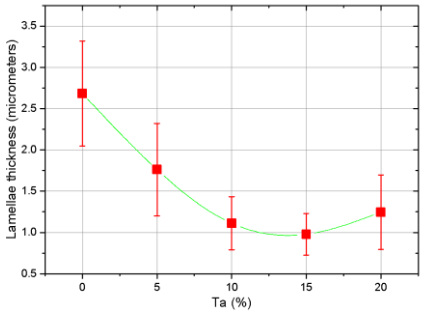

Fig. 3 Lamellae thickness of α phase variation in respect to tantalum content measured on light microscopy micrographs

Since a change in thickness of the α lamellae was observed, an analysis in this respect was performed using the following procedure: on 5 light microscopy micrographs the largest thickness of 10 random chosen lamellae was measured, totaling 50 measurements/alloy. The results were the averaged and the lamellae thickness variation in respect to tantalum content was plotted, as presented in fig. 3.

As tantalum content increases the thickness of the α lamellae tends to decrease, according to the variation presented in fig. 3. When no tantalum was added (alloy A1), an average lamellae thickness of 2.68±0.63μm was determined, in the measurements a maximum of 3.86μm and minimum of 1.57 μm were found. At 5%Ta (alloy A2), the average thickness decreased to 1.76±0.56μm, with a maximum of 4.46 μm and minimum 0f 1.08 μm. At 10%Ta (alloy A3) a further decrease in lamellae thickness is observed, averaging at 1.11±0.32μm, with a maximum of 2.02 μm and a minimum of 0.54 μm. The addition of 15%Ta in the alloy (alloy A4) leads to further decrease in the lamellae thickness that averages at 0.98±0.25μm, the maximum of 1.54 μm and minimum of 0.57 μm being recorded in the measurements performed. At highest concentration of tantalum (alloy A5) the average α lamellae thickness tends to increase, averaging at 1.25±0.45μm. This increase is caused by the appearance of thick α plates in the microstructure (as

observed in fig. 2.e.), as the maximum thickness measured was 3.66μm and the minimum 0.69 μm.

The same procedure applied on light microscopy micrographs was applied for the micrographs obtained by scanning electron microscopy depicted in fig. 4.

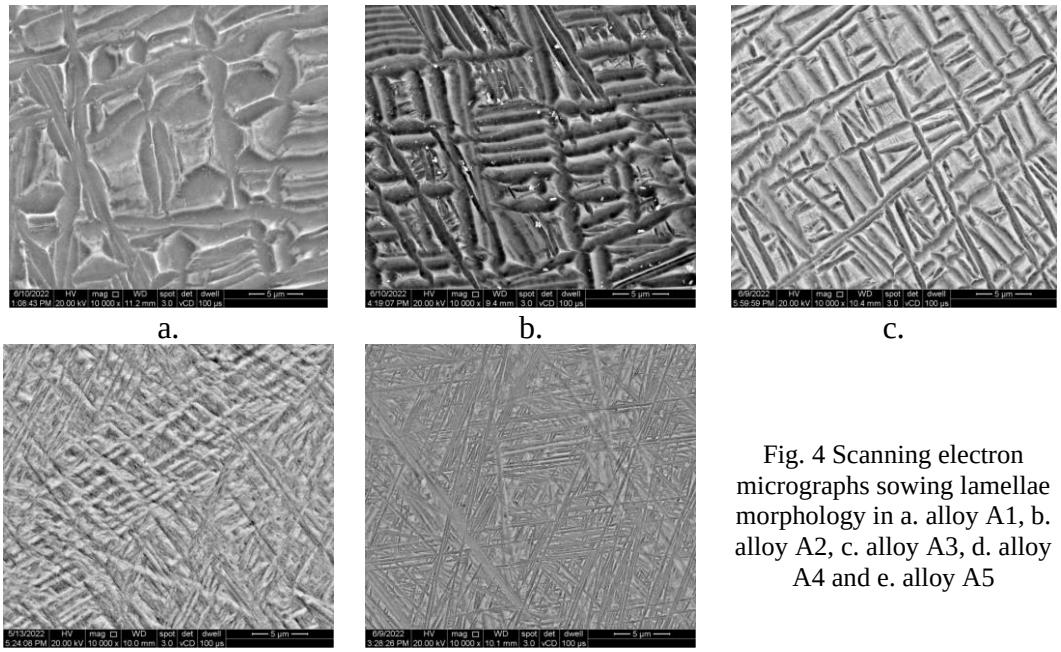

Fig. 4 Scanning electron micrographs sowing lamellae morphology in a. alloy A1, b. alloy A2, c. alloy A3, d. alloy A4 and e. alloy A5

The morphology of α phase presented in fig. 4 reveals its transition from the Widmanstatten one (for α+β alloys) in fig. 4.a. and b. towards lamellar as colonies (fig. 4. c. and d.) or rosettes (fig. 4. e.) [34-37]. As for the thickness variation in respect to tantalum addition, the plot presented in fig. 5 shows a similar trend as the one observed in the study performed on light microscopy micrographs.

As the examined surface by SEM is reduced, the probability to encounter large α plates is decreased, still there is a good similarity with the results obtained with the study on light micrographs.

Further studies were aimed at a constituent proportion quantification using the volume method, as described in following paragraph.

The constituent proportions were determined by placing a grid on the captured and binarized microstructure (for a better distinction between the two constituents present). The points where the vertical and horizontal lines of the grid intersected were counted and attributed to one of the constituents (α phase - light appearance and β phase - dark appearance). The proportions were then estimated by computing the ratio between the number of points that fell on one constituent to the total number of points of the grid. The analysis was repeated on 15 random

fields on each sample and the results averaged with the variation of α and β in respect to tantalum content plotted in fig. 6.

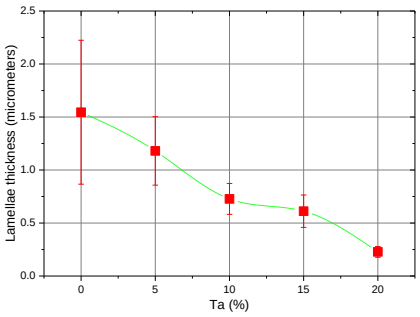

Fig. 5 Lamellae thickness of α phase variation in respect to tantalum content measured on scanning electron microscopy micrographs

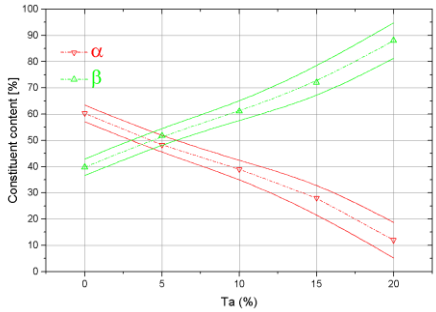

Fig. 6 The variation of α and β in respect to tantalum content. The bands represent ±1 standard deviation

The addition of tantalum increases the β phase proportion as it is a β stabilizing element. With no tantalum addition the alloy starts with roughly 60% α and this content gradually decreases down to 12% α at 20% tantalum. At 5%Ta a roughly 50%α - 50% β structure is obtained.

The results fit into values reported by Wang [38], Zhou [39] and Gao [40].

3.4 Vickers Hardness

The Vickers hardness tests were performed on two regions of the cast ingots: Region 1 designates a central position in respect to the longitudinal section of the ingot, while Region 2 designates a region close to the edge of the ingot (obviously, respecting the specification of the standard regarding distances from the edge of the sample). On each experimental alloy five hardness measurements were performed, and the results were then averaged. In fig. 7 the hardness variation in respect to tantalum content is depicted.

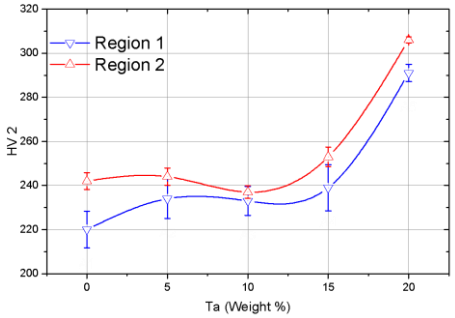

Fig. 7 Vickers hardness variation in respect to tantalum content

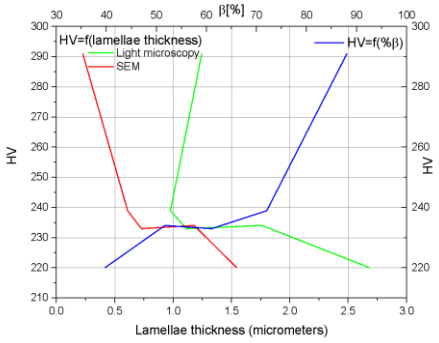

Fig. 8 Hardness variation in respect to lamellae thickness

The hardness variation is similar for both regions, with slight differences that can be attributed to the microstructure: the region adjacent to the edge of the ingot (Region 2) has a higher thermal gradient and the result is a finer microstructure than the one in the center of the ingot, where the grains are coarse.

The addition of tantalum has no significant effect on hardness value up to 15%. A major influence is observed at 20%Ta concentration.

For Region 1 the alloy with no tantalum has an average hardness of 220HV and a slight increase in hardness (circa 14HV) was observed at 5%Ta. The increase to 10%Ta had no effect on hardness value and at 15%Ta the hardness increased by circa 20HV. At 20%Ta the hardness increases by circa 70HV.

In Region 2 the alloy with no tantalum has an average value of 242HV, and in this case there is no variation up to 15%Ta, where an increase by roughly 11HV is observed. The most significant increase is achieved at 20%Ta, when the hardness increases by circa 64HV.

The plot in fig. 8 is constructed using hardness data from Region 1 since all microstructure studies (including lamellae thickness measurements) were performed on samples obtained from the center of the ingots. The hardness appears to be influenced by lamellae thickness and constituent content, as α lamellae thickness increases, the hardness value decreases, and, as β phase content increases so does the average hardness value.

4. Conclusions

The five experimental alloys in the Ti-Nb-Ta-Zr-Ag system with various tantalum concentrations were studied as cast to observe the changes in microstructure. The addition of 20% increases the alloy density by roughly 27% in respect to the alloy without tantalum, limiting its use to small components.

The chemical compositions obtained for the experimental alloys matches in a large extent the desired one, the resulting alloys having a satisfactory homogeneous chemical composition.

The structure of the alloys is comprised of α and β phases with varying proportions. The addition of tantalum increases the proportion of β phase, from 40% when no tantalum was added to 80% when 20%Ta was added. The microstructure is initially typical Widmanstatten for α+β alloys up to 10%Ta, above this concentration the α phase shows a lamellar structure, organized as colonies or rosettes.

The thickness of α lamellae appears to be greatly influenced by tantalum addition.

The hardness appears to be influenced by α lamellae thickness and content of β as tantalum concentration exceeds 15%.

This study of the alloys in as cast condition is relevant for the use of the alloys in dentistry, where processing route is limited to casting of the implant.

Acknowledgment

This work has been funded by the European Social Fund from the Sectoral Operational Programme Human Capital 2014-2020, through the Financial Agreement with the title "Training of PhD students and postdoctoral researchers in order to acquire applied research skills - SMART", Contract no. 13530/16.06.2022 - SMIS code: 153734.

R E F E R E N C E S

[1]. *Bai, L.; Gong, C.; Chen, X. H.; Sun, Y. X.; Zhang, J. F.; Cai, L. C.; Zhu, S. Y.; Xie, S. Q.*: Additive Manufacturing of Customized Metallic Orthopedic Implants: Materials, Structures, and Surface Modifications. Metals-Basel 2019, 9

[2]. *Lange, G.; Ungethum, M.:* Metallic Materials for Surgical Implants. Z Metallkd 1986, 77, 545-552

[3]. *Rho, J. Y.; Tsui, T. Y.; Pharr, G. M.*: Elastic properties of human cortical and trabecular lamellar bone measured by nanoindentation. Acs Sym Ser 1997, 18, 1325-1330

[4]. *Kennady, M. C.; Tucker, M. R.; Lester, G. E.; Buckley, M. J.*: Stress Shielding Effect of Rigid Internal-Fixation Plates on Mandibular Bone-Grafts - a Photon-Absorption Densitometry and Quantitative Computerized Tomographic Evaluation. Int J Oral Max Surg 1989, 18, 307-310

[5]. *Gheorghe, D.; Pop, D.; Ciocoiu, R.; Trante, O.; Milea, C.; Mohan, A.; Benea, H.; Saceleanu, V.*: Microstructure Development in Titanium and Its Alloys Used for Medical Applications. U Politeh Buch Ser B 2019, 81, 243-258

[6]. *Zhao, Q. Y.; Bolzoni, L.; Chen, Y. N.; Xu, Y. K.; Torrens, R.; Yang, F.*: Processing of metastable beta titanium alloy: Comprehensive study on deformation behaviour and exceptional microstructure variation mechanisms. J Mater Sci Technol 2022, 126, 22-43

[7]. *Kudrman, J.; Fousek, J.; Brezina, V.; Mikova, R.; Vesely, J.*: Titanium alloys for implants in medicine. Kovove Mater 2007, 45, 199-208

[8]. *Kuroda, D.; Niinomi, M.; Morinaga, M.; Kato, Y.; Yashiro, T.*: Design and mechanical properties of new beta type titanium alloys for implant materials. Mat Sci Eng a-Struct 1998, 243, 244-249

[9]. *Steinemann, S. G.; Mausli, P. A.; Szmuklermoncler, S.; Semlitsch, M.; Pohler, O.; Hintermann, H. E.; Perren, S. M.*: Beta-Titanium Alloy for Surgical Implants. Titanium '92: Science and Technology, Vols 1-3 1993, 2689-2696

[10]. *Rechtin, J.; Torresani, E.; Ivanov, E.; Olevsky, E.*: Fabrication of Titanium-Niobium-Zirconium-Tantalium Alloy (TNZT) Bioimplant Components with Controllable Porosity by Spark Plasma Sintering. Materials 2018, 11

[11]. *Niinomi, M.*: Mechanical biocompatibilities of titanium alloys for biomedical applications. J Mech Behav Biomed 2008, 1, 30-42

[12]. *Narita, K., Niinomi, M., Nakai, M., Akahori, T., Tsutsumi, H., Oribe, K., ... & Sato, S.* (2009). Mechanical properties of implant rods made of low-modulus β-type titanium alloy, Ti-29Nb-13Ta-4.6 Zr, for spinal fixture. In 2008 Materials Science and Technology Conference, MS and T'08 (pp. 83-90). American Ceramic Society

[13]. *Chuanyuan Mao, Weijun Yu, Min Jin, Yingchen Wang, Xiaoqing Shang, Lu Lin, Xiaoqin Zeng, Liqiang Wang, Eryi Lu,* Mechanobiologically optimized Ti–35Nb–2Ta–3Zr improves load transduction and enhances bone remodeling in tilted dental implant therapy, Bioactive Materials, **Volume 16**, 2022, Pages 15-26, ISSN 2452-199X, https://doi.org/10.1016/j.bioactmat.2022.03.005

[14]. *Edamatsu, H., Kawai, T., Matsui, K., Nakai, M., Takahashi, T., Echigo, S., ... & Kamakura, S.* (2015). High bone bonding ability and affinity of new low-rigidity β-type Ti-29Nb-13Ta-4.6 Zr alloy as a dental implant. J. Dent. Oral Health, 7, 2-8

[15]. *Shi, A. Q.; Cai, D. G.; Hu, J. L.; Zhao, X. T.; Qin, G. W.; Han, Y.; Zhang, E. L.:* Development of a low elastic modulus and antibacterial Ti-13Nb-13Zr-5Cu titanium alloy by microstructure controlling. Mat Sci Eng C-Mater 2021, 126

[16]. *Donaghy, C. L.; McFadden, R.; Kelaini, S.; Carson, L.; Margariti, A.; Chan, C. W.*: Creating an antibacterial surface on beta TNZT alloys for hip implant applications by laser nitriding. Opt Laser Technol 2020, 121

[17]. *Liu, H.; Liu, R.; Ullah, I.; Zhang, S. Y.; Sun, Z. Q.; Ren, L.; Yang, K.*: Rough surface of copper-bearing titanium alloy with multifunctions of osteogenic ability and antibacterial activity. J Mater Sci Technol 2020, 48, 130-139

[18]. *Li, X.; Chen, T.; Hu, J.; Li, S. J.; Zou, Q.; Li, Y. F.; Jiang, N.; Li, H.; Li, J. H.*: Modified surface morphology of a novel Ti-24Nb-4Zr-7.9Sn titanium alloy via anodic oxidation for enhanced interfacial biocompatibility and osseointegration. Colloid Surface B 2016, 144, 265-275

[19]. *Fu, J. N.; Liu, X. M.; Tan, L.; Cui, Z. D.; Liang, Y. Q.; Li, Z. Y.; Zhu, S. L.; Zheng, Y. F.; Yeung, K. W. K.; Chu, P. K.; Wu, S. L.*: Modulation of the mechanosensing of mesenchymal stem cells by laser-induced patterning for the acceleration of tissue reconstruction through the Wnt/beta-catenin signaling pathway activation. Acta Biomater 2020, 101, 152-167

[20]. *Chan, C. W.*: Creating an antibacterial surface on beta TNZT alloys for hip implant applications by laser nitriding. Opt Laser Technol 2020, 121

[21]. *Kawakami, H.; Yoshida, K.; Nishida, Y.; Kikuchi, Y.; Sato, Y.*: Antibacterial properties of metallic elements for alloying evaluated with application of JIS Z 2801 : 2000. Isij Int 2008, 48, 1299-1304

[22]. *Oh, K. T., Joo, U. H., Park, G. H., Hwang, C. J., & Kim, K. N.* (2006). Effect of silver addition on the properties of nickel–titanium alloys for dental application. Journal of Biomedical Materials Research Part B: Applied Biomaterials: An Official Journal of The Society for Biomaterials, The Japanese Society for Biomaterials, and The Australian Society for Biomaterials and the Korean Society for Biomaterials, 76(2), 306-314

[23]. *Rahnejat, B.; Nemati, N. H.; Sadrnezhaad, S. K.; Shokrgozar, M. A.*: Promoting osteoblast proliferation and differentiation on functionalized and laser treated titanium substrate using hydroxyapatiteβ-tricalcium phosphate/silver nanoparticles. Mater Chem Phys 2023, 293

[24]. *Cazzola, M.; Barberi, J.; Ferraris, S.; Cochis, A.; Cempura, G.; Czyrska-Filemonowicz, A.; Rimondini, L.; Spriano, S.*: Bioactive Titanium Surfaces Enriched with Silver Nanoparticles Through an In Situ Reduction: Looking for a Balance Between Cytocompatibility and Antibacterial Activity. Adv Eng Mater 2022

[25]. *Diez-Escudero, A.; Carlsson, E.; Andersson, B.; Jarhult, J. D.; Hailer, N. P.*: Trabecular Titanium for Orthopedic Applications: Balancing Antimicrobial with Osteoconductive Properties by Varying Silver Contents. Acs Appl Mater Inter 2022

[26]. *San, H. S.; Paresoglou, M.; Minneboo, M.; van Hengel, I. A. J.; Yilmaz, A.; Gonzalez-Garcia, Y.; Fluit, A. C.; Hagedoorn, P. L.; Fratila-Apachitei, L. E.; Apachitei, I.; Zadpoor, A. A.*: Fighting Antibiotic-Resistant Bacterial Infections by Surface Biofunctionalization of 3D-Printed Porous Titanium Implants with Reduced Graphene Oxide and Silver Nanoparticles. Int J Mol Sci 2022, 23

[27]. *Haugen, H. J.; Makhtari, S.; Ahmadi, S.; Hussain, B.*: The Antibacterial and Cytotoxic Effects of Silver Nanoparticles Coated Titanium Implants: A Narrative Review. Materials 2022, 15

[28]. *Pencea, I.; Branzei, M.; Turcu, R. N.; Sfat, C. E.*: New Approach for Chemical Homogeneity Analysis of an AISI 316L Stainless Steel Bar Batch. Rev Chim-Bucharest 2018, 69, 1079-1083

[29]. *Cristescu, I.; Antoniac, I.; Branzei, M.; Ghiban, B.; Ciocoiu, R.; Ciuca, I.; Semenescu, A.; Gradinaru, S.; Pop, D.; Raiciu, A. D.*: Fractography Study of Explanted Intramedullary Nails. Mater Plast 2019, 56, 759-773

[30]. *Li, B. Q.; Li, C. L.; Wang, Z. X.; Lu, X.*: Preparation of Ti-Nb-Ta-Zr alloys for load-bearing biomedical applications. Rare Metals 2019, 38, 571-576

[31]. *Li, B. Q.; Li, X. C.; Lu, X.*: Microstructure and compressive properties of porous Ti-Nb-Ta-Zr alloy for orthopedic applications. J Mater Res 2019, 34, 4045-4055

[32]. *Li, B. Q.; Xie, R. Z.; Lu, X.*: Microstructure, mechanical property and corrosion behavior of porous Ti-Ta-Nb-Zr. Bioact Mater 2020, 5, 564-568

[33]. *Preisler, D.; Strasky, J.; Harcuba, P.; Kosutova, T.; Dopita, M.; Janovska, M.; Hajek, M.; Janecek, M.*: Phase transformations in Ti-Nb-Zr-Ta-O β titanium alloys with high oxygen and reduced Nb and Ta content. Acta Crystallogr A 2021, 77, C1251-C1251

[34]. *Tang, B.; Kou, H. C.; Zhang, X.; Gao, P. Y.; Li, J. S.*: Study on the formation mechanism of α lamellae in a near β titanium alloy. Prog Nat Sci-Mater 2016, 26, 385-390

[35]. *Zheng, H. J.; Fan, X. G.; Zeng, X.; Zuo, R.*: Crystal orientation and morphology of α lamellae in wrought titanium alloys: On the role of microstructure evolution in β processing. Chinese J Aeronaut 2019, 32, 1305-1313

[36]. *Harcuba, P.; Smilauerova, J.; Holy, V.*: α phase lamellae orientation relationship in metastable β titanium alloys. Acta Crystallogr A 2021, 77, C1253-C1253

[37]. *Pang, H. Y.; Luo, J.; Li, C.; Li, M. Q.*: The role of β phase in the morphology evolution of α lamellae in a dual-phase titanium alloy during high temperature compression. J Alloy Compd 2022, 910

[38]. *Wang, Q. J.; Wu, J. C.; Tong, L. B.; Wang, W.; Yin, R. K.; Cao, P.*: Phase Transformation and Kinetics in Metastable β Titanium Alloy During Isothermal Treatment. Adv Eng Mater 2021, 23

[39]. *Zhou, L. B.; Sun, J. S.; Zhang, R. Z.; Chen, J.; He, J. J.; Yuan, T. C.*: A new insight into the α phase precipitation in β titanium alloy. Vacuum 2021, 189

[40]. *Gao, X. X.; Zhang, S. F.; Wang, L.; Yang, K.; Wang, P.; Chen, H. Y.*: Evolution of grain boundary α phase during cooling from β phase field in a α plus β titanium alloy. Mater Lett 2021, 301